INTERNATIONAL JOURNAL OF HEAT AND TECHNOLOGY

ISSN: 0392-8764
Vol. 35, No. 4, December 2017, pp. 893-902
DOI: 10.18280/ijht.350426

A publication of IIETA

IIETA International Information and Engineering Technology Association
Advancing the World of Information and Engineering
http://www.iieta.org/Journals/IJHT

Magnetohydrodynamic flow of brinkman-type engine oil based MoS_2-nanofluid in a rotating disk with hall effect

Farhad Ali[1,2,3], Bibi Aamina[3], Ilyas Khan[4], Nadeem A. Sheikh[1,2,3] Muhammad Saqib[1,2,3]

[1] Computational Analysis Research Group, Ton Duc Thang University, Ho Chi Minh, 700000, Vietnam
[2] Faculty of Mathematics and Statistics, Ton Duc Thang University, Ho Chi Minh 700000 Vietnam
[3] Department of Mathematics, City University of Science and Information Technology, Peshawar 25000, Pakistan
[4] Basic Engineering Sciences Department, College of Engineering Majmaah University, Majmaah 11952, Saudi Arabia

Email: farhad.ali@tdt.edu.vn

ABSTRACT

Nanotechnology currently has an important role in reducing engine wear and improving fuel efficiency within engines using nanoparticles in engine oil. Therefore, the work reported in this paper, aims to investigate the magnetohydrodynamic (MHD) flow of Brinkman-type Engine Oil-based Molybdenum disulfide (MoS_2) nanofluid (BEOBMN) in a rotating frame along with Hall effect and thermal radiation. The problem is modeled in terms of partial differential equations with physical initial and boundary conditions. The Laplace transform technique is used to evaluate the exact solutions for velocity and temperature profiles. Graphical results are obtained through a computational software Mathcad and discussed for various embedded parameters. The Skin-friction and Nusselt number are computed in the tabular form and it is noticed that the rate of heat transfer enhances 6.35% by adding MoS_2 in engine oil which improved its lubrication.

Keywords: BEOBMN, MHD Flow, Closed-form Solutions, The Laplace Transform.

1. INTRODUCTION

Convective heat transfer in nanofluids has gotten great concern in science as well as in engineering. Traditional fluids such as kerosene oil, ethylene glycol, polyethylene glycol, water and engine-oil etc. play a vital role in thermal transport application but these fluids have poor thermal conductivities which degrade the heat transfer rate. Despite the substantial attempts to upgrade the rate of heat transfer by the extended surfaces usage, mini-channels, and micro-channels, more improvement in heating and cooling is always in demand [1]. Early studies, carried out by using millimeter or micrometer particles dispersed in traditional heat transfer fluids. This idea of utilizing small-sized solid particles within the base fluid to enhance their thermal conductivity and heat transfer rate was given by Maxwell [2]. However, there were some limitations of Maxwell's idea i.e. the faster settling time, clogging micro-channels of devices, abrasion of surfaces and erosion of pipelines etc. [3]. In 1995 Choi [4], introduced a new idea of suspension of nano-sized particles in the base fluids to improve the thermal conductivity. Alongside higher thermal conductivity, the suspension of nano-sized particles instead micro-sized particles in a traditional base fluid (currently known as nanofluids) is preferred because of some valid scientific reasons such as longer suspension time (more stable), lower clogging and erosion, lower demand for significant energy saving pumping power. Nanofluids, due to high thermal conductivity have several useful and potential applications in physical circumstances. For example, they are used on a large scale in automobiles as a coolant, microelectronics, and microchips in computer, biomedicines, fuel cells, transportation, food processing, and solid-state lighting and manufacturing. In inclusion metals and metallic oxides, carbon nanotubes are used for heat transfer enhancement, biomedical equipment, lubrication in moving parts of machines [5-6]. Loganathan et al. [7] presented the first exact solution of nanofluids for unsteady free convection flow, taken into account the effect of radiation. Sheikholeslami et al. [8] investigated the MHD flow of nanofluid and heat transfer in a rotating frame along with the effect of Brownian motion. Recently, the effect of gold (Au) nanoparticles on hydromagnetic poiseuille flow of nanofluid embedded in a porous medium have been investigated by Aman et al. [9]. Of course, the list of such studies can continue, but we close it

with some of the most interesting analytical and numerical results that have been obtained in [10–16].

Nowadays, different nanoparticles with various shapes are used as additives for improving properties of lubricants. In present work, spherical shape MoS_2 nanoparticles have been used in EO because MoS_2 has low friction properties and robustness which can help in enhancing the heat transfer rate as well as lubricity of engine oil [17 &18]. Molybdenum disulfide (MoS_2) is an inorganic compound classified as a metal dichalcogenide, an alternate layer of molybdenum and sulfur atoms. It is a silvery black solid that occurs as the mineral molybdenite. MoS_2 is relatively unreactive and is unaffected by dilute acids and oxygen. Each molybdenum atom is sandwich between trigonal prisms of sulfur atoms in a hexagonal closed pack arrangement. The sheets of sulfur are loosely bound by van der Waals interactions [19]. The homogenous stable Newtonian molybdenum disulfide MoS_2 nanofluids were experimentally prepared by Zhang et al. [20]. Similar to graphene, MoS_2 has single and multilayer sheets with large bandgap structure. MoS_2 has attracted the interest of researchers due to its promising applications in many areas especially, in two-dimensional electronic devices such as Field Effect Transistors (FETs). Due to this special structure, it has been extensively applied to logic circuits and amplifier devices [21 & 22]. Some other attempts on MoS_2 nanofluids are made by Gul et al. [23], Kato et al. [24] and Mao et al. [25]. The heat capacity, thermal conductivity, and volumetric thermal expansion coefficients were experimentally studied by Liu et al. [26] and Ding and Xiao [27].

In 1856 Darcy proposed a model for the fluid that flows over a body with low porosity [28]. The flow passes over a body with high porosity does not obey Darcy's law. This model was recommended by Brinkman for fluid that passing through high porous media in 1949 [29]. There is a massive use of Brinkman-type flow in many branches of engineering and science e.g., groundwater hydrology, reservoir engineering, soil science, soil mechanics and chemical engineering [30]. Brinkman in his pioneering work [31], presented calculations for the viscous forces exerted by fluid flowing on a dense swarm of particles. Another model, developed by Brinkman [32] for the incompressible viscous fluid passing through a porous media, which incorporates Darcy's equation as a unique case. Several researchers have done informative works on Brinkman-type fluid, which are listed in the references [33-36]. Recently, Ali et al. [37] used the Laplace transform technique to develop several new exact solutions for the flow of Brinkman-type fluid. The solutions were obtained in the simple form of complementary and elementary error functions. In another paper, Ali et al. [38] obtained closed-form solutions for unsteady free convection hydromagnetic flow of an incompressible Brinkman-type fluid by using the Laplace transform technique, four different types of flows were discussed in this paper along with thermal radiation. Recently, Ali et al. [39] considered the flow of Brinkman-type fluid with four different types of nanoparticles in a spherical shape. Exact solutions were obtained for velocity, temperature and concentration profiles by using the Laplace transforms.

In recent years, the study of hydromagnetic is under great concerned. It has many important applications in engineering and technology such as hydromagnetic generators (it includes disk system) and MHD flow meters, plasma studies, pumps, bearings, geothermal energy extractions and nuclear reactors, solar energy collection, boundary layer control, aerodynamic heating casting and levitation, extraction of petroleum products and cooling of an infinite metallic plate in a cooling bath. Besides this, there are many applications of hydromagnetic flow of non-Newtonian fluids in a rotating body in metrology, geographic, turbomachinery, astrophysical and several other areas. In addition, it has many applications in biomedical such as blood flow in capillaries, dialysis of blood in artificial kidney and flow in blood oxygenation. Also, it has many applications in engineering such as in transpiration cooling, porous pipe design and design of filters [40].

It is greatly defined that ionized fluid having low density and strong magnetic field, the Hall current become more notable. Hall effects on MHD flow have many applications as recognized by many researchers which are used in engineering which comprises of underground energy storage system, MHD power generation, Hall current accelerators, nuclear power reactors, magnetometers and spacecraft propulsion etc. Some of the important investigations are given in the references [41-44]. Furthermore, both Hall current and rotation induce secondary flow in the fluid flow. Some important investigations have been done on the effects of thermal radiation on Hydromagnetic flow and heat transfer problems. It has many applications such as nuclear plants, gas turbines, aircraft, different propulsion devices, satellites, missiles, and space vehicles and at an industrial level as well as in engineering areas thermal radiation effect become important for high operating temperatures [45].

However, none of these papers took into consideration the rotating flow of Brinkman-type nanofluids. Therefore, the objective of this work is to fill this gap. More exactly, our analysis is focused on the study of the impact of Hall current and thermal radiation on the MHD flow of Brinkman-type engine oil based MoS_2 nanofluid in a rotating disk. The problem is presented in the form of partial differential equations along with physical boundary conditions. The Laplace transform technique has been used to get the closed-form solutions for velocity and temperature profiles. The results have been discussed for several embedded parameters. From the present study, it is noticed that the rate of heat transfer enhances 6.35% by adding MoS_2 in engine oil which improved its lubrication. Furthermore, the results from the present study for nanofluids may use for industrial and automobile cooling which could result in great energy savings and in emission reduction.

2. MATHEMATICAL MODELING

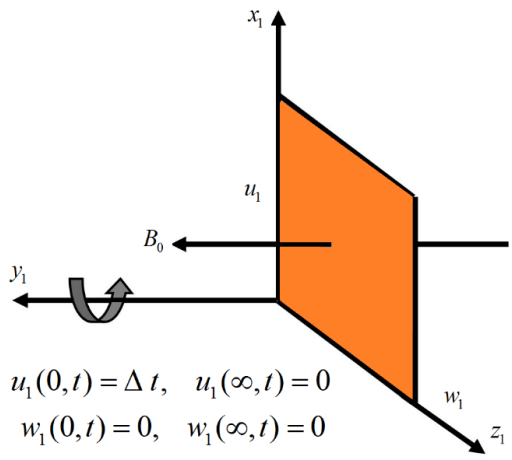

Figure 1.The illustrative diagram of the problem

Consider an incompressible MoS_2-EO-based Brinkman-type nanofluid with spherical shape nanoparticles in a rotating frame. Rotation of the fluid is about y_1-axis. The fluid is assumed to be electrically conducted, the Hall effect is also taken into account. Heat transfer along with thermal radiation is also considered. Initially, the fluid is at rest with ambient temperature $T_{1\infty}$. At the time $t = 0^+$ the plate starts motion with a variable velocity of constant amplitude U_0. The temperature of the plate is raised to T_{1w} and then remains constant. The geometry of the problem is shown in Figure1.

Under the above assumptions, the governing equations for MHD convective flow of Brinkman-type nanofluid in a rotating frame with Hall effect, taking thermal radiation into account and under Boussinesq's approximation, are given by:

$$\frac{\partial u_1}{\partial t_1} + \beta u_1 - 2\Omega w_1 = \frac{\mu_{nf}}{\rho_{nf}}\frac{\partial^2 u_1}{\partial y_1^2} - \frac{\sigma_{nf} B_0^2 (u_1 + m w_1)}{\rho_{nf}(1+m^2)} + g\beta_{nf}(T_1 - T_{1\infty}) \quad (1)$$

$$\frac{\partial w_1}{\partial t_1} + \beta w_1 + 2\Omega u_1 = \frac{\mu_{nf}}{\rho_{nf}}\frac{\partial^2 w_1}{\partial y_1^2} + \frac{\sigma_{nf} B_0^2 (m u_1 - w_1)}{\rho_{nf}(1+m^2)} \quad (2)$$

$$(\rho c_p)_{nf}\frac{\partial T_1}{\partial t_1} = k_{nf}\frac{\partial^2 T_1}{\partial y_1^2} - \frac{\partial q_{1r}}{\partial y_1} \quad (3)$$

subject to the following initial and boundary conditions:

$$\left.\begin{array}{c} u_1(y,0) = 0, \quad u_1(0,t) = \Delta t, \quad u_1(\infty,t) = 0 \\ w_1(y,0) = 0, \quad w_1(0,t) = 0, \quad w_1(\infty,t) = 0 \\ T_1(y,0) = T_{1\infty}, T_1(0,t) = T_{1\infty} + (T_{1w} - T_{1\infty})At, T_1(\infty,t) = T_{1\infty} \end{array}\right\}. \quad (4)$$

The temperature on the wall is dependent on time, which means the variable temperature is considered on the boundary.

For the nanofluids, the expressions of ρ_{nf}, μ_{nf}, σ_{nf}, $(\rho\beta)_{nf}$ and $(\rho c_p)_{nf}$ are given as

$$\rho_{nf} = (1-\phi)\rho_f + \phi\rho_s,\ \mu_{nf} = \mu_f(1-\phi)^{-2.5},$$
$$(\rho\beta)_{nf} = (1-\phi)(\rho\beta)_f + \phi(\rho\beta)_s,$$
$$(\rho c_p)_{nf} = (1-\phi)(\rho c_p)_f + \phi(\rho c_p)_s,$$
$$\sigma_{nf} = \sigma_f\left[1 + \frac{3(\sigma-1)\phi}{(\sigma+2)-(\sigma-1)\phi}\right],$$
$$\sigma = \frac{\sigma_s}{\sigma_f},\quad k_{nf} = k_f\left[\frac{k_s + 2k_f - 2\phi(k_f - k_s)}{k_s + 2k_f + \phi(k_f - k_s)}\right],$$

According to Oztop and Abu-Nada [46], the expressions which are presented above are restricted to spherical shaped nanoparticles and the thermophysical properties of base fluid and nanoparticle are given in Table 1.

Considering small temperature difference between fluid temperature and free stream temperature, can be linearized by using Taylor series about the free stream temperature. Neglecting second and higher order terms in

Table 1. Thermophysical properties of EO and MoS_2 [6]

	ρ (K gm^{-3})	C_P (JKg^{-1}K^{-1})	K (Wm^{-1} K^{-1})	β $\times10^{-5}$ (K^{-1})
ENGINE OIL	863	2048	0.1404	0.00007
MOS_2	5.06×10^3	397.21	904.4	2.8424

We adopt the Roseland's approximation for radiative flux q_{1r} namely:

$$q_{1r} = \frac{-4\sigma^*}{3k^*}\frac{\partial T_1^4}{\partial y_1}, \quad (5)$$

$(T_1 - T_{1\infty})$, we get:

$$T_1^4 = 4T_{1\infty}^3 T_1 - 3T_{1\infty}^4.$$

Using above in equation (5), we get

$$q_{1r} = \frac{-4\sigma^*}{3k^*}\frac{\partial(4T_{1\infty}^3 T_1 - 3T_{1\infty}^4)}{\partial y_1},$$

As $T_{1\infty}^4$ is a constant temperature, therefore, $\frac{\partial T_{1\infty}^4}{\partial y_1} = 0$, we have

$$q_{1r} = \frac{-16T_{1\infty}^3\sigma^*}{3k^*}\frac{\partial T_1}{\partial y_1}. \quad (6)$$

substituting equation (6) into equation (3), we get

$$(\rho c_p)_{nf}\frac{\partial T_1}{\partial t_1} = k_{nf}\frac{\partial^2 T_1}{\partial y_1^2} + \frac{16T_{1\infty}^3\sigma^*}{3k^*}\frac{\partial^2 T_1}{\partial y_1^2}. \quad (7)$$

introducing the following dimensionless variables

$$u = \frac{u_1}{u_0},\quad y = \frac{u_0}{\nu}y_1,\quad t = \frac{u_0^2}{\nu}t_1,\quad w = \frac{w_1}{u_0},\quad T = \frac{T_1 - T_{1\infty}}{T_{1w} - T_{1\infty}},$$

into equations (1), (2) and (7) reduce to dimensionless equations (8), (9) and (10) respectively,

$$\frac{\partial u}{\partial t} + \beta_1 u - 2\eta w = \frac{1}{\mathrm{Re}}\frac{\partial^2 u}{\partial y^2} - M_0\left(\frac{u + mw}{1+m^2}\right) + Gr_o T, \quad (8)$$

$$\frac{\partial w}{\partial t} + \beta_1 w + 2\eta u = \frac{1}{\mathrm{Re}}\frac{\partial^2 w}{\partial y^2} + M_0\left(\frac{mu - w}{1+m^2}\right), \quad (9)$$

$$\frac{\partial T}{\partial t} = \frac{1}{\mathrm{Pr}_{eff}}\frac{\partial^2 T}{\partial y^2}, \quad (10)$$

subject to the dimensionless initial and boundary conditions:

$$\left.\begin{aligned} &u(y,0)=0,\ u(0,t)=\xi t,\ u(\infty,t)=0\\ &w(y,0)=0,\ w(0,t)=0,\ w(\infty,t)=0\\ &T(y,0)=0,\ T(0,t)=t,\ \ T(\infty,t)=0 \end{aligned}\right\}, \tag{11}$$

where

$$\begin{aligned} &\beta_1=\frac{\beta\nu}{u_0^2},\eta=\frac{\Omega w}{u_0^2},Re=(1-\phi)^{2.5}\left[(1-\phi)+\phi\left(\frac{\rho_s}{\rho_f}\right)\right],\\ &\phi_2=\frac{(1-\phi)\rho_f+\phi\rho_s\left(\frac{\beta_s}{\beta_f}\right)}{(1-\phi)\rho_f+\phi\rho_s},\varphi_3=(1-\phi)+\phi\frac{(\rho c_p)_s}{(\rho c_p)_f},\\ &M=\frac{\sigma_f\nu B_0^2}{\rho_f u_0^2},\ M_0=\frac{M\phi_1(1-\phi)^{2.5}}{\mathrm{Re}},Gr=\frac{g\beta_f\nu(T_1-T_{1\infty})}{u_0^3},\\ &Gr_0=Gr\phi_2,\ \phi_1=1+\frac{3(\sigma-1)\phi}{(\sigma+2)-(\sigma-1)\phi},\ \mathrm{Pr}=\frac{(\mu c_p)_f}{k_f},\\ &Nr=\frac{16\sigma^*T_{1\infty}^3}{3k^*k_f},\quad \lambda_{nf}=\frac{k_{nf}}{k_f},\quad \mathrm{Pr}_{eff}=\frac{\mathrm{Pr}\,\phi_3}{(\lambda_{nf}+Nr)}, \end{aligned} \tag{12}$$

where $\varphi_i(i=1,2,3)$ represent the functions which depend on the thermo-physical properties of the base fluid and nanoparticles. According to the geometry, equations (8) to (10) are the governing equations of the considered flow regime subjected to the initial and boundary conditions (11). We now take a particular case of interest, namely, uniformly accelerated the movement of the plate i.e. $\Delta(t)=\xi t$ where ξ is dimensionless constant, to understand the flow features of the fluid flow. Equations (8 and 9) can be expressed in more suitable form as

$$\frac{\partial F}{\partial t}=\frac{1}{\mathrm{Re}}\frac{\partial^2 F}{\partial y^2}-\lambda F+Gr_0T\ , \tag{13}$$

where $F=u+wi$ is a complex velocity and $\lambda=M_0\,\frac{(1-mi)}{1+m^2}+\beta_1+2k^2i$ is a constant.

The dimensionless initial and boundary conditions are:

$$\left.\begin{aligned} &F(y,0)=0,\ \ T(y,0)=0\\ &F(0,t)=\xi t,\ \ T(0,t)=t\\ &F(\infty,t)=0,\ \ T(\infty,t)=0 \end{aligned}\right\}. \tag{14}$$

3. SOLUTION OF THE GOVERNING PROBLEM

The Laplace transform technique has been used to obtain the closed-form solutions for the partial differential equations (10 and 13).

3.1 Calculation of temperature distribution

Apply the Laplace transform technique to equation (10) using the corresponding initial and boundary conditions from equation (14), we get

$$\overline{T}(y,s)=\frac{1}{s^2}e^{-y\sqrt{\mathrm{Pr}_{eff}\,s}}. \tag{15}$$

Now by taking Laplace inverse of equation (15), we get

$$T(y,t)=F_4\left(y\sqrt{\mathrm{Pr}_{eff}},t\right). \tag{16}$$

3.2 Calculation of velocity distribution

Apply the Laplace transform technique to equation (13) and using corresponding initial conditions from equation (14), we get

$$\frac{d^2\overline{F}}{dy^2}-\mathrm{Re}(\lambda+s)\overline{F}(y,s)+\mathrm{Re}\,Gr_0\overline{T}(y,s)=0. \tag{17}$$

Now substituting equation (15) into equation (17) and using the corresponding boundary conditions from equation (14), the solution of equation (17) becomes

$$\begin{aligned} \overline{F}(y,s)=&\left[\frac{\xi}{s^2}-\frac{Gr_2}{s^2}+\frac{Gr_2}{b_1(s-b_1)}-\frac{Gr_2}{b_1s}\right]e^{-y\sqrt{\mathrm{Re}}\sqrt{\lambda+s}}\\ &-\left[\frac{Gr_2}{b_1(s-b_1)}-\frac{Gr_2}{s^2}-\frac{Gr_2}{b_1s}\right]e^{-y\sqrt{\mathrm{Pr}_{eff}\,s}}, \end{aligned} \tag{18}$$

where

$$b_1=\frac{\mathrm{Re}\,\lambda}{\mathrm{Pr}_{eff}-\mathrm{Re}},\quad Gr_1=\frac{\mathrm{Re}\,Gr_0}{\mathrm{Pr}_{eff}-\mathrm{Re}}\ \text{ and }\ Gr_2=\frac{Gr_1}{b_1}.$$

Now finally applying the inverse Laplace transform to equation (18), we get

$$\begin{aligned} F(y,t)=&\xi F_1\left(y\sqrt{\mathrm{Re}},t,\lambda\right)-Gr_2F_1\left(y\sqrt{\mathrm{Re}},t,\lambda\right)\\ &+\frac{Gr_2}{b_1}F_2\left(y\sqrt{\mathrm{Re}},t,b_1,\lambda\right)-\frac{Gr_2}{b_1}F_3\left(y\sqrt{\mathrm{Re}},t,\lambda\right)\\ &-\frac{Gr_2}{b_1}F_6\left(y\sqrt{\mathrm{Pr}_{eff}},t,b_1\right)+Gr_2F_4\left(y\sqrt{\mathrm{Pr}_{eff}},t\right)\\ &+\frac{Gr_2}{b_1}F_5\left(y\sqrt{\mathrm{Pr}_{eff}},t\right). \end{aligned} \tag{19}$$

The expressions for $F_i\left(i=1,2,...6\right)$ are given in Appendices.

3.3 Special case

By taking $\beta_1\to 0$, $\lambda=M_0\,\frac{(1-mi)}{1+m^2}+2k^2i$, equation (18) is reduced to the following form

$$\begin{aligned} F(y,t)=&\xi F_1\left(y\sqrt{\mathrm{Re}},t,\lambda\right)-Gr_2F_1\left(y\sqrt{\mathrm{Re}},t,\lambda\right)\\ &+\frac{Gr_2}{b_1}F_2\left(y\sqrt{\mathrm{Re}},t,b_1,\lambda\right)-\frac{Gr_2}{b_1}F_3\left(y\sqrt{\mathrm{Re}},t,\lambda\right)\\ &-\frac{Gr_2}{b_1}F_6\left(y\sqrt{\mathrm{Pr}_{eff}},t,b_1\right)+Gr_2F_4\left(y\sqrt{\mathrm{Pr}_{eff}},t\right)\\ &+\frac{Gr_2}{b_1}F_5\left(y\sqrt{\mathrm{Pr}_{eff}},t\right), \end{aligned} \tag{20}$$

which is the solution for Newtonian nanofluid in a rotating frame.

3.4 Skin friction and Nusselt number

The skin-friction and Nusselt number are defined as:
The expression for dimensionless skin friction is given as

$$C_f = \frac{1}{(1-\phi)^{2.5}} \frac{\partial F(y,t)}{\partial y}\bigg|_{y=0} = \frac{1}{(1-\phi)^{2.5}} L^{-1}\left\{\lim_{y\to 0} \frac{\partial F(y,s)}{\partial y}\right\}. \quad (21)$$

The dimensionless Nusselt number is given by

$$\mathrm{Nu} = -\frac{k_{nf}}{k_f} \frac{\partial T(y,t)}{\partial y}\bigg|_{y=0} = -\left[\frac{k_s + 2k_f - 2\phi\left(k_f - k_s\right)}{k_s + 2k_f + \phi\left(k_f - k_s\right)}\right] L^{-1}\left\{\lim_{y\to 0} \frac{\partial T(y,s)}{\partial y}\right\}. \quad (22)$$

4. RESULTS AND DISCUSSION

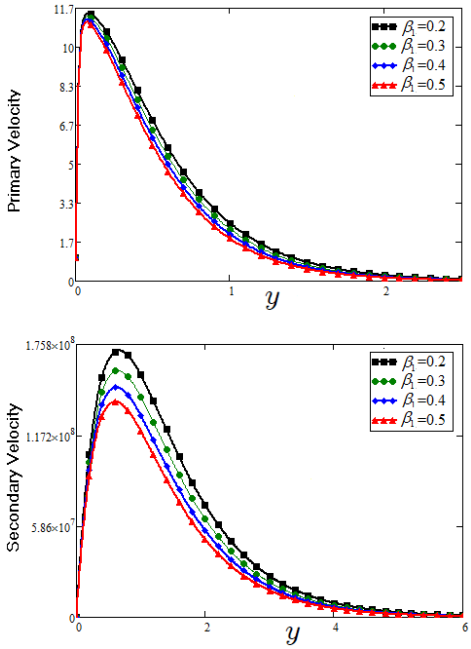

Figure 2. Velocity profile of MoS2-EO-based Brinkman type nanofluid for different values of β_1 when $\phi = 0.03$, $Gr = 0.4$, $\mathrm{Pr} = 1000$, $m = 0.5$, $\eta = 0.2$, $M = 1$, $t = 1$, $Nr = 0.2$

In this section, the analytical results are plotted graphically for embedded parameters using computational software MATHCAD. Different graphs are shown for this purpose. These graphs show the influence of Brinkman parameter β_1, magnetic parameter M, volume fraction ϕ, Hall effect m, Grashof number Gr, thermal radiation Nr and rotation parameter η on primary and secondary velocities. Additionally, the effects of thermal radiation Nr and volume fraction ϕ are shown in temperature distribution.

Figure2 has been plotted to show the influence of Brinkman parameter β_1 on fluid velocities (Primary and Secondary), it is observed that $\beta_1 = 0.2$ have greater fluid velocity than $\beta_1 = 0.5$. Physically, it is true because Brinkman parameter β_1 is a ratio between drag forces and density, so by increasing β_1 drag forces increased which cause a decrease in velocity.

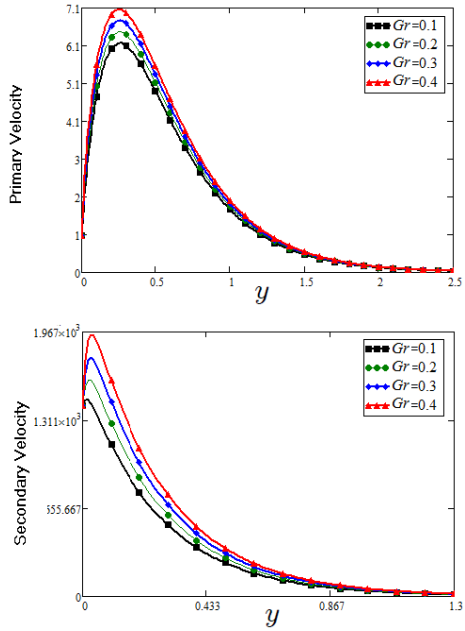

Figure 3. Velocity profile of MoS_2-EO-based Brinkman type nanofluid for different values of Gr when $\phi = 0.03$, $\beta_1 = 0.5$, $\mathrm{Pr} = 1000$, $m = 0.5$, $\eta = 0.2$, $M = 1$, $t = 1$, $Nr = 0.2$

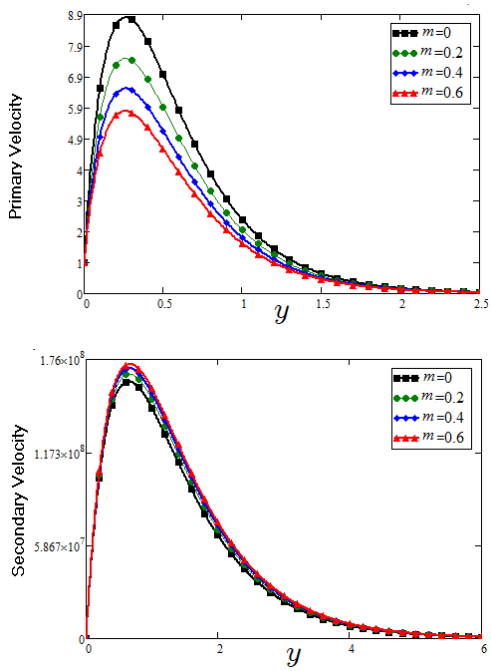

Figure 4. Velocity profile of MoS_2-EO-based Brinkman type nanofluid for different values of m when $\phi = 0.03$, $\beta_1 = 0.5$, $\mathrm{Pr} = 1000$, $Gr = 0.4$, $\eta = 0.2$, $M = 1$, $t = 1$, $Nr = 0.2$

The effect of thermal Grashof number Gr on secondary and primary velocities has been portrayed in figure 3. It is noticed that both velocities raised by increasing the values of Gr. This behavior is obvious because it is the ratio of

buoyancy forces and viscous forces so by increasing the values of Gr from 0.1 to 0.4, it increases the buoyancy forces and consequently velocities increase.

Figure 4 depicts the effect of Hall current parameter m on primary and secondary velocities. The figure illustrated that for $m=0$ the velocity is greater than $m=0.6$, which shows that Hall current decelerates the primary fluid velocity. Whereas, it has an opposite effect on the secondary fluid velocity. Secondary fluid velocity enhanced for higher values of m.

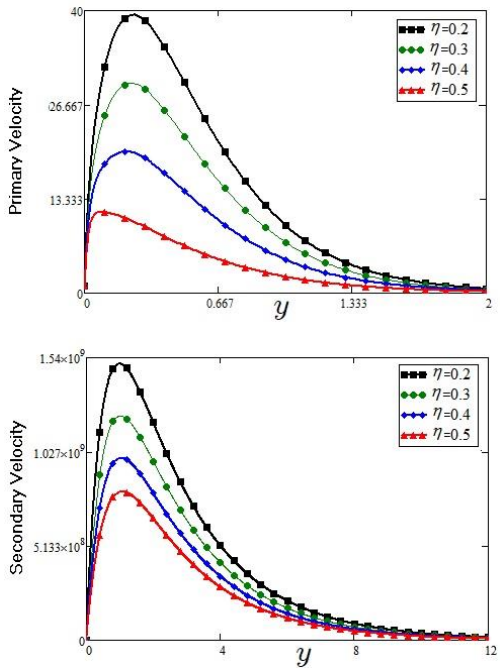

Figure 5. Velocity profile of MoS_2-EO-based Brinkman type nanofluid for different values of η when $\phi=0.03,\ \beta_1=0.5,$ $\Pr=1000,\ Gr=0.4,\ m=0.5,\ M=1,\ t=1,\ Nr=0.2$

Figure6 is plotted to present the effect of M on primary and secondary velocity profiles. The results show that by applying high magnetic field strength, both the primary and secondary velocities become decreased, this is an obvious result because magnetic field raises the Lorentz forces of an electrically conducted fluid which tends to slow down the motion of the fluid in the boundary layer.

The outcomes for rotation parameter η can be seen in figure 5, it is observed that the primary and secondary velocities decrease for higher values of η. Although it is the fact that Coriolis forces have a tendency to decrease the primary flow and increases the secondary flow, the behavior of secondary flow is not obvious so in the present case, the secondary flow is decreased by increasing the value of η.

The influence of volume fraction ϕ on the velocity of fluid flow has been illustrated in figure 7. The range of nanoparticles volume fraction is taken between $0\le\phi\le0.04$ because if the volume fraction exceeds from 0.04 then the problem of sedimentation arises. From figure 7, it is observed that when ϕ is increased from 0.01 to 0.04, both the primary and secondary velocities are decreased. Large values of ϕ enhancing the viscous forces due to which fluid velocity is decreased. A decrease in the velocity means that the viscosity of EO is increased which consequently increase the boiling and freezing point of the EO due to which the lubrication properties of EO become more effective and efficient.

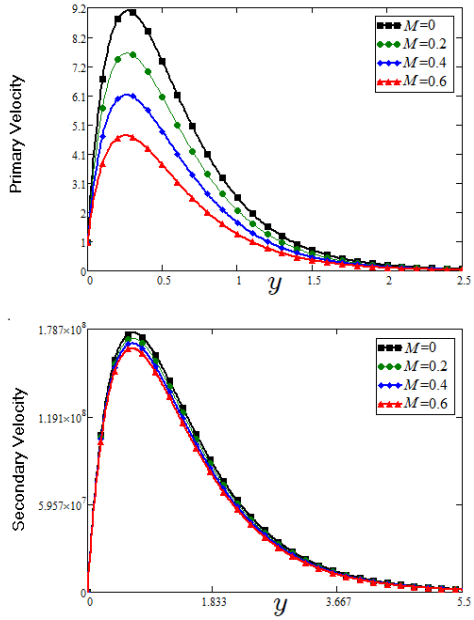

Figure 6. Velocity profile of MoS_2-EO-based Brinkman type nanofluid for different values of M when $\phi=0.03,\ \beta_1=0.5,$ $\Pr=1000,\ Gr=0.4,\ \eta=0.2,\ m=0.5,\ t=1,\ Nr=0.2$

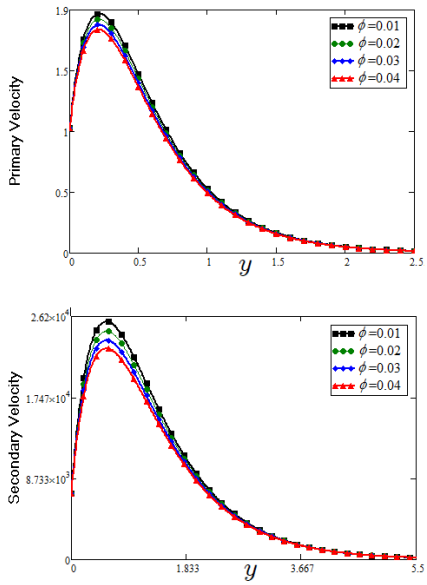

Figure 7. Velocity profile of MoS_2-EO-based Brinkman type nanofluid for different values of ϕ when $\beta_1=0.5,\ \Pr=1000,$ $m=0.5,\ Gr=0.4,\ \eta=0.2,\ M=1,\ t=1,\ Nr=0.2$

Figure. 8 highlights the influence of thermal radiation Nr on the fluid velocity, which shows that by increasing the values of Nr both primary and secondary velocities are enhanced.

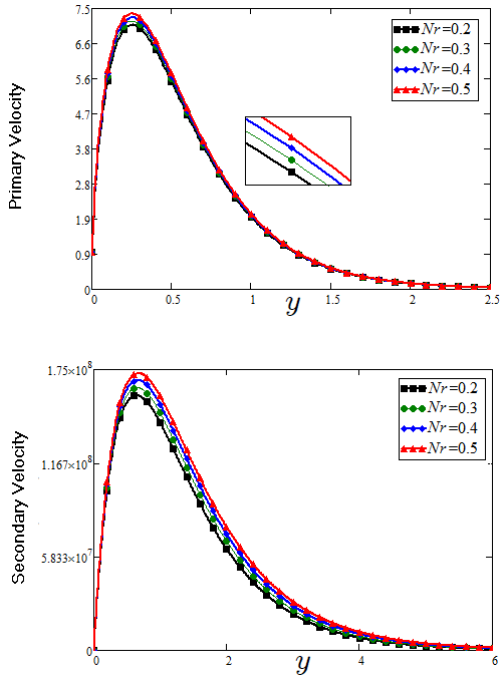

Figure 8. Velocity profile of MoS_2-EO-based Brinkman type nanofluid for different values of Nr when $\phi = 0.03$, $\beta_1 = 0.5$, $\Pr = 1000, m = 0.5,\ Gr = 0.4,\ \eta = 0.2,\ M = 1,\ t = 1$

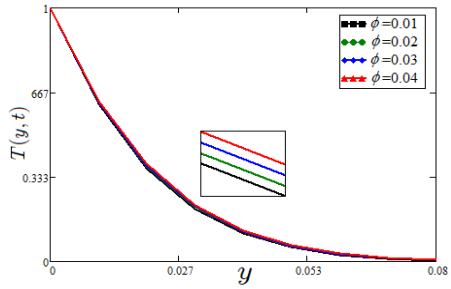

Figure 9. Temperature profile of MoS_2-EO-based Brinkman type nanofluid for different values of ϕ when $\Pr = 1000,\ t = 1,\ Nr = 0.2$

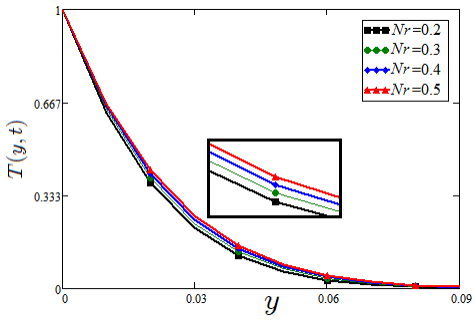

Figure 10. Temperature profile of MoS_2-EO-based Brinkman type nanofluid for different values of Nr when $\Pr = 1000,\ t = 1,\ \phi = 0.03$

In figure 9 the effect of nanoparticle volume fraction is noticed on the temperature profile, that is, an increase in nanoparticle volume fraction causes an increase in temperature due to shear thinning behaviour.

The influence of thermal radiation parameter Nr on temperature has been illustrated in figure 10, which shows the rise in velocity as we increase the value of Nr .

Table 2. shows the effect of various parameters on skin friction, by taking higher values of M, η, t, Gr and Nr, skin friction increases.

Table 2. Effect of various parameters on skin friction coefficient (c_f)

ϕ	M	Pr	m	η	t	Gr	Nr	β_1	C_f
0.03	1	1000	0.5	0.2	1	5	0.2	0.5	10.747
0.04	1	1000	0.5	0.2	1	5	0.2	0.5	10.572
0.03	**1.5**	1000	0.5	0.2	1	5	0.2	0.5	24.204
0.03	1	**1500**	0.5	0.2	1	5	0.2	0.5	10.724
0.03	1	1000	**0.7**	0.2	1	5	0.2	0.5	5.768
0.03	1	1000	0.5	**0.4**	1	5	0.2	0.5	93.253
0.03	1	1000	0.5	0.2	**1.5**	5	0.2	0.5	20.052
0.03	1	1000	0.5	0.2	1	**6**	0.2	0.5	10.712
0.03	1	1000	0.5	0.2	1	5	**0.4**	0.5	10.757
0.03	1	1000	0.5	0.2	1	5	0.2	**0.7**	10.592

Table 3 shows that Nusselt number is increased by increasing the values of ϕ. Whereas Pr increases the Nusselt number while decreases the skin friction.

Table 3. Effect of various parameters on Nusselt number (Nu)

ϕ	Nr	Pr	t	Nu
0.03	0.2	1000	1	34.151
0.03	**0.4**	1000	1	31.618
0.03	0.2	**1500**	1	38.662
0.03	0.2	1000	**1.5**	41.826

Table 4. Impact of volume fraction on nusselt number and percent enhancment

ϕ	Nr	Pr	t	Nu	% Enhancement
0	0.2	1000	1	32.603	-
0.01	0.2	1000	1	33.115	1.57
0.02	0.2	1000	1	33.631	3.15
0.03	0.2	1000	1	34.151	4.74
0.04	0.2	1000	1	34.674	6.35

Table 4 shows the impact of volume fraction on the Nusselt number. From Table 4 it observed that at zero volume fraction the Nusselt number is 32.603 and by increasing the volume fraction up to 0.04 the rate of heat transfer enhances up to

6.35 % .from here it can be concluded that the engine oil-based MoS_2 nanofluid is thermally more stable, has more effectitive lubrication properties and has efficient heat transfer rate as compare to the regular engine oil.

5. CONCLUSIONS

In recent years, many lubricants with different properties are produced to be used in various mechanical systems including internal combustion engines. Friction in mechanical systems is the main factor for energy loss and lubrication is one of the most effective ways of reducing friction. Engine oil (EO) is one of the most used lubricants in internal combustion engines, which power cars, motorcycles, engine-generators, and many other machines. Hence, improving lubricant properties of EO is always been in demand. From last few decades, nanofluids are categorized as a new low friction technology, and a method to reduce wear properties. Therefore, in the present work, Spherical shaped MoS_2 nanoparticles are used in EO, which is taken as a base fluid. More exactly, this work investigates for the first time the MHD flow of Brinkman-type nanofluid in a rotating frame with Hall-effect. Molybdenum disulfide nanoparticles of spherical shape are dispersed in EO to enhance its thermal conductivity. Exact solutions are developed for velocity and temperature via the Laplace transform technique. The important points from this study are summarized in the following:

- By increasing the values of ϕ, β_1, η and M, decreased the nanofluid primary and secondary velocities.
- With increasing values of m, the primary velocity is decreased whereas the secondary velocity is increased.
- Temperature is increased with increasing values of ϕ and Nr.
- Skin friction is found as the increasing function of M, η, t, Gr and Nr.
- The Nusselt number/heat transfer rate increased with increasing values of ϕ.
- Pr increases the Nusselt number while decreased the skin friction.
- Heat transfer rate of EO-based nanofluid is 6.35% greater as compared to regular EO fluid.

REFERENCES

[1] Das K. (2014). Flow and heat transfer characteristics of nanofluids in a rotating frame, *Alexandria Engineering Journal*, Vol. 53, No. 3, pp. 757-766. DOI: 10.1016/j.aej.2014.04.003

[2] Maxwell J.C. (1881). *A Treatise on Electricity and Magnetism*, Clarendon Press, London, pp. 120-141.

[3] Gul A., Khan I., Shafie S., Khalid A., Khan A. (2015). Heat transfer in MHD mixed convection flow of a ferrofluid along a vertical channel, *PloS One*, Vol. 10, No. 11, pp. 1-14. DOI: 10.1371/journal.pone.0141213

[4] Choi S.U.S. (1995). Enhancing thermal conductivity of fluids with nanoparticles, *ASME-Publications-Fed*, Vol. 231, No. 2, pp. 99-106.

[5] Das K. (2014). Flow and heat transfer characteristics of nanofluids in a rotating frame, *Alexandria Engineering Journal*, Vol. 53, No. 3, pp. 757-766. DOI: 10.1016/j.aej.2014.04.003

[6] Jan S.A.A., Ali F., Sheikh N.A., Khan I., Saqib M., Gohar M. (2017). Engine oil based generalized brinkman-type nano-liquid with molybdenum disulphide nanoparticles of spherical shape: Atangana-Baleanu fractional model, *Numerical Methods for Partial Differential Equations*, pp. 1-23. DOI: 10.1002/num.22200

[7] Loganathan P., Nirmal C.P., Ganesan P. (2013). Radiation effects on an unsteady natural convective flow of a nanofluid past an infinite vertical plate, *Nano*, Vol. 8, No. 1, pp. 1-10. DOI: 10.1142/S179329201350001X

[8] Sheikholeslami M., Ganji D.D. (2014). Three-dimensional heat and mass transfer in a rotating system using nanofluid, *Powder Technology*, Vol. *253*, No. 2, pp. 789-796. DOI: 10.1016/j.powtec.2013.12.042

[9] Aman S., Khan I., Ismail Z., Salleh M.Z. (2016). Impacts of gold nanoparticles on MHD mixed convection Poiseuille flow of nanofluid passing through a porous medium in the presence of thermal radiation, thermal diffusion and chemical reaction, *Neural Computing and Applications*, pp. 1-9. DOI: 10.1007/s00521-016-2688-7

[10] Harish S., Ishikawa K., Einarsson E., Aikawa S., Inoue T., Zhao P., Maruyama S. (2012). Temperature-dependent thermal conductivity increases of aqueous nanofluid with single-walled carbon nanotube inclusion, *Materials Express*, Vol. 2, No. 3, pp. 213-223. DOI: 10.1166/mex.2012.1074

[11] Rashidi M.M., Abelman S., Mehr N.F. (2013). Entropy generation in steady MHD flow due to a rotating porous disk in a nanofluid, *International Journal of Heat and Mass Transfer*, Vol. 62, pp. 515-525. DOI: 10.1016/j.ijheatmasstransfer.2013.03.004

[12] Hosseini S.M., Moghadassi A.R., Henneke D., Elkamel A. (2010). The thermal conductivities enhancement of mono-ethylene glycol and paraffin fluids by adding β-SiC nanoparticles, *Journal of Thermal Analysis and Calorimetry*, Vol. 101, No. 1, pp. 113-118. DOI: 10.1007/s10973-009-0498-1

[13] Xuan Y., Li Q. (2000). Heat transfer enhancement of nanofluids, *International Journal of Heat and Fluid Flow*, Vol. 21, No. 1, pp. 58-64. DOI: 10.1016/S0142-727X(99)00067-3

[14] Putra N., Thiesen P., Roetzel W. (2003). Temperature dependence of thermal conductivity enhancement for nanofluids, *Journal of Heat Transfer*, Vol. 125, No. 4, pp. 567-574. DOI: 10.1115/1.1571080

[15] Huminic G., Huminic A. (2012). Application of nanofluids in heat exchangers: A review, *Renewable and Sustainable Energy Reviews*, Vol. 16, No. 8, pp. 5625-5638. DOI: 10.1016/j.rser.2012.05.023

[16] Aaiza G., Khan I., Shafie S. (2015). Energy transfer in mixed convection MHD flow of nanofluid containing different shapes of nanoparticles in a channel filled with a saturated porous medium, *Nanoscale Research Letters*, Vol. 10, No. 1, pp. 1-14. DOI: 10.1186/s11671-015-1144-4

[17] Radisavljevic B., Radenovic A., Brivio J., Giacometti I.V., Kis A. (2011). Single-layer MoS2 transistors, *Nature Nanotechnology*, Vol. 6, No. 3, pp. 147-150. DOI: 10.1038/nnano.2010.279

[18] Radisavljevic B., Whitwick M.B., Kis A. (2011). Integrated circuits and logic operations based on single-layer MoS2, *ACS Nano*, Vol. 5. No. 12, pp. 9934-9938. DOI**:** 10.1021/nn203715c

[19] Khan I. (2017). Shape effects of MoS2 nanoparticles on MHD slip flow of molybdenum disulfide nanofluid in a porous medium, *Journal of Molecular Liquids*, Vol. 233, pp. 442-451. DOI: 10.1016/j.molliq.2017.03.009

[20] Zhang Y., Gu S., Yan B., Ren J. (2012). Solvent-free ionic molybdenum disulfide (MoS2) nanofluids, *Journal of Materials Chemistry*, Vol. 22, No. 30, pp. 14843-14846. DOI: 10.1039/C2JM33106C

[21] Das S., Chen H.Y., Penumatcha A.V., Appenzeller J. (2012). High-performance multilayer MoS2 transistors with scandium contacts, *Nano Letters*, Vol. 13, No. 1, pp. 100-105. DOI: 10.1021/nl303583v

[22] Dankert A., Langouche L., Kamalakar M.V., Dash S.P. (2014). High-performance molybdenum disulfide field-effect transistors with spin tunnel contacts, *ACS Nano*, Vol. 8, No. 1, pp. 476-482. DOI: 10.1021/nn404961e

[23] Gu S., Zhang Y., Yan B. (2013). Solvent-free ionic molybdenum disulfide (MoS 2) nanofluids with self-healing lubricating behaviors, *Materials Letters*, Vol. 97, pp. 169-172. DOI: 10.1016/j.matlet.2013.01.058

[24] Kato H., Takama M., Iwai Y., Washida K., Sasaki Y. (2003). Wear and mechanical properties of sintered copper–tin composites containing graphite or molybdenum disulfide, *Wear*, Vol. 255, No. 1, pp. 573-578. DOI: 10.1016/S0043-1648(03)00072-3

[25] Mao C., Huang Y., Zhou X., Gan H., Zhang J., Zhou Z. (2014). The tribological properties of nanofluid used in minimum quantity lubrication grinding, *The International Journal of Advanced Manufacturing Technology*, Vol. 71, No. 5-8, pp. 1221-1228. DOI: 10.1007/s00170-013-5576-7

[26] Liu J., Choi G.M., Cahill D.G. (2014). Measurement of the anisotropic thermal conductivity of molybdenum disulfide by the time-resolved magneto-optic Kerr effect, *Journal of Applied Physics*, Vol. 116, No. 23, pp. 233107. DOI: 10.1063/1.4904513

[27] Ding Y., Xiao B. (2015). Thermal expansion tensors, Grüneisen parameters and phonon velocities of bulk MT 2 (M= W and Mo; T= S and Se) from first principles calculations, *RSC Advances*, Vol. 5, No. 24. pp. 18391-18400. DOI: 10.1039/C4RA16966B

[28] Simmons C.T. (2008). Henry Darcy (1803–1858): Immortalised by his scientific legacy, *Hydrogeology Journal*, Vol. 16, No. 6, p. 1023. DOI: 10.1007/s10040-008-0304-3

[29] Khaled A.R., Vafai K. (2003). The role of porous media in modeling flow and heat transfer in biological tissues, *International Journal of Heat and Mass Transfer*, Vol. 46, No. 26, pp. 4989-5003. DOI: 10.1016/S0017-9310(03)00301-6

[30] Bear J. (2013). *Dynamics of Fluids in Porous Media*, Courier Corporation, New York.

[31] Brinkman H.C. (1949). A calculation of the viscous force exerted by a flowing fluid on a dense swarm of particles, *Flow, Turbulence and Combustion*, Vol. 1, No. 1, pp. 27. DOI: 10.1007/BF02120313

[32] Brinkman H.C. (1949). On the permeability of media consisting of closely packed porous particles, *Flow, Turbulence and Combustion*, Vol. 1, No. 1, pp. 81. DOI: 10.1007/BF02120318

[33] Fetecau, C., Fetecau, C., & Imran, M. A. (2011). On Stokes problems for fluids of Brinkman type, *Mathematical Reports*, Vol. 13, No. 1, pp. 15-26.

[34] Hill A.A. (2004). Convection induced by the selective absorption of radiation for the Brinkman model, *Continuum Mechanics and Thermodynamics*, Vol. 16. No. 1, pp. 43-52. DOI: 10.1007/s00161-003-0140-6

[35] Gorla R.S.R., Mansour M.A., Sahar M.G. (1999). Natural convection from a vertical plate in a porous medium using Brinkman's model, *Transport in Porous Media*, Vol. 36, No. 3, pp. 357-371. DOI: 10.1023/A:1006593330865

[36] Rajagopal K.R. (2007). On a hierarchy of approximate models for flows of incompressible fluids through porous solids, *Mathematical Models and Methods in Applied Sciences*, Vol. 17, No. 2, pp. 215-252. DOI: 10.1142/S0218202507001899

[37] Ali F., Khan I., Shafie S. (2012). A note on new exact solutions for some unsteady flows of Brinkman-type fluids over a plane wall, *Zeitschrift für Naturforschung A*, Vol. 67, No. 6-7, pp. 377-380. DOI: 10.5560/zna.2012-0039

[38] Ali F., Khan I., Ul H.S., Shafie S. (2013). Influence of thermal radiation on unsteady free convection MHD flow of Brinkman type fluid in a porous medium with Newtonian heating, *Mathematical Problems in Engineering*, Vol. 2013, pp. 1-13. DOI: 10.1155/2013/632394

[39] Ali F., Gohar M., Khan I. (2016). The MHD flow of water-based Brinkman type nanofluid over a vertical plate embedded in a porous medium with variable surface velocity, temperature and concentration, *Journal of Molecular Liquids*, Vol. 223, pp. 412-419. DOI: 10.1016/j.molliq.2016.08.068

[40] Sarkar S., Seth G.S. (2016). Unsteady hydromagnetic natural convection flow past a vertical plate with time-dependent free stream through a porous medium in the presence of hall-current, rotation, and heat absorption, *Journal of Aerospace Engineering*, Vol. 30, No. 1. DOI: 10.1061/(ASCE)AS.1943-5525.0000672

[41] Seth G.S., Kumbhakar B., Sarkar S. (2016). Unsteady MHD natural convection flows with exponentially accelerated free-stream past a vertical plate in the presence of Hall current and rotation, *Rendiconti del Circolo Matematico di Palermo*, Vol. 66, No. 3, pp. 263-288. DOI: 10.1007/s12215-016-0250-1

[42] Aboeldahab E.M., Elbarbary E.M. (2001). Hall current effect on magnetohydrodynamic free convection flows past a semi-infinite vertical plate with mass transfer, *International Journal of Engineering Science*, Vol. 39, No. 14, pp. 1641-1652. DOI: 10.1016/S0020-7225(01)00020-9

[43] Ali F., Sheikh N.A., Saqib M., Khan I. (2017). The unsteady MHD flow of second-grade fluid over an oscillating vertical plate with isothermal temperature in

[44] a porous medium with heat and mass transfer by using the laplace transform technique, *Journal of PorousMedia*, Vol. 20, No. 8, pp. 671-690. DOI: 10.1615/JPorMedia.v20.i8.10

[45] Sutton G.W., Sherman A. (1965). *Engineering Magnetohydrodynamics*, Courier Dover Publications, US.

[46] Das K. (2012). Impact of thermal radiation on MHD slip flow over a flat plate with variable fluid properties, *Heat and Mass Transfer*, Vol. 48, No. 5, pp. 767-778. DOI: 10.1007/s00231-011-0924-3

[47] Oztop H.F., Abu-Nada E. (2008) Numerical study of natural convection in partially heated rectangular enclosures filled with nanofluids, *International Journal of Heat Fluid Flow*, Vol. 29, No. 5, pp. 1326-1336. DOI: 10.1016/j.ijheatfluidflow.2008.04.009

NOMENCLATURE

A constant with dimension $\frac{1}{s}$ and shows the amplitude

B_0 induced magnetic field;

g acceleration due to gravity (m s^{-2});

u' nanofluid velocity in x'-direction (m/s);

w' nanofluid velocity in z'-direction (m/s);

m Hall current parameter

Gr Grashof number

k_f the thermal conductivity of the base fluid ($Wm^{-1}K^{-1}$);

k_{nf} the thermal conductivity of nanofluid ($Wm^{-1}K^{-1}$);

k_s the thermal conductivity of nanoparticles ($Wm^{-1}K^{-1}$);

k^* mean absorption coefficient;

μ_{nf} dynamic viscosity of nanofluid (kg m^{-1} s^{-1});

q_{1r} radiative heat flux (=W m^{-2});

T_1 fluid temperature (K);

β_f the thermal expansion coefficient of base fluid (K^{-1});

β_{nf} the thermal expansion coefficient of nanofluid (K^{-1});

β_s the thermal expansion coefficient of nanoparticle (K^1);

Ω rotation parameter;

μ_f viscosity of base fluid (kg m^{-1} s^{-1});

ϕ the solid volume fraction of the nanoparticle;

ρ_f the density of the base fluid (kg m^{-3});

ρ_{nf} the density of nanofluid (kg m^{-3});

$(\rho c_p)_f$ heat capacitance of base fluid;

$(\rho c_p)_{nf}$ heat capacitance of nanofluid;

$(\rho c_p)_s$ heat capacitance of nanoparticle;

σ^* Stefan-Boltzmann constant ($=5.67\times10^{-8}$ W/m^2K^4);

σ_f electrical conductivity of base fluid (=s^3 A^2 $m^{-3}kg^{-1}$);

σ_{nf} electrical conductivity of nanofluid (=s^3 A^2 $m^{-3}kg^{-1}$);

σ_s electrical conductivity of nanoparticle (=s^3 A^2 $m^{-3}kg^{-1}$).

ν_f dynamic viscosity coefficient of base fluid;

β_1 Brinkman parameter;

η rotation parameter;

M magnetic parameter;

Gr Grashof number;

Pr Prandtl number;

Nr radiation parameter;

η Dimensionless rotation parameter;

APPENDIX

$$\overline{F_1}(y,s,H)=L^{-1}\left[\frac{1}{s^2}e^{-y\sqrt{H+s}}\right]=F_1(y,t,H)=\begin{bmatrix}e^{-y\sqrt{H}}\operatorname{erfc}\left(\frac{y}{2\sqrt{t}}-\sqrt{Ht}\right)\left(\frac{t}{2}-\frac{y}{4\sqrt{H}}\right)\\+e^{y\sqrt{H}}\operatorname{erfc}\left(\frac{y}{2\sqrt{t}}+\sqrt{Ht}\right)\left(\frac{t}{2}+\frac{y}{4\sqrt{H}}\right)\end{bmatrix}$$

$$\overline{F_2}(y,s,b,M)=L^{-1}\left[\frac{1}{s-b}e^{-y\sqrt{M+s}}\right]=F_2(y,t,b,M)=\frac{e^{bt}}{2}\begin{bmatrix}e^{-y\sqrt{M+b}}\operatorname{erfc}\left(\frac{y}{2\sqrt{t}}-\sqrt{(b+M)t}\right)\\+e^{y\sqrt{M+b}}\operatorname{erfc}\left(\frac{y}{2\sqrt{t}}+\sqrt{(b+M)t}\right)\end{bmatrix}$$

$$\overline{F_3}(y,s,M)=L^{-1}\left[\frac{1}{s}e^{-y\sqrt{M+s}}\right]=F_3(y,t,M)=\frac{1}{2}\begin{bmatrix}e^{-y\sqrt{M}}\operatorname{erfc}\left(\frac{y}{2\sqrt{t}}-\sqrt{Mt}\right)\\+e^{y\sqrt{M+b}}\operatorname{erfc}\left(\frac{y}{2\sqrt{t}}+\sqrt{Mt}\right)\end{bmatrix}$$

$$\overline{F_4}(y,s)=L^{-1}\left[\frac{1}{s^2}e^{-y\sqrt{s}}\right]=F_4(y,t)=\left[\left(t+\frac{y^2}{2}\right)\operatorname{erfc}\left(\frac{y}{2\sqrt{t}}\right)-\frac{y\sqrt{t}}{\sqrt{\pi}}e^{\frac{y^2}{4t}}\right]$$

$$\overline{F_5}(y,s)=L^{-1}\left[\frac{1}{s}e^{-y\sqrt{s}}\right]=F_5(y,t)=\operatorname{erfc}\left(\frac{y}{2\sqrt{t}}\right)$$

$$\overline{F_6}(y,s,b)=L^{-1}\left[\frac{1}{s-b}e^{-y\sqrt{s}}\right]=F_6(y,t,b)=\frac{e^{bt}}{2}\begin{bmatrix}e^{-y\sqrt{b}}\operatorname{erfc}\left(\frac{y}{2\sqrt{t}}-\sqrt{bt}\right)\\+e^{y\sqrt{b}}\operatorname{erfc}\left(\frac{y}{2\sqrt{t}}+\sqrt{bt}\right)\end{bmatrix}$$